Ternary Choline Chloride–Monoethanolamine Based Deep Eutectic Solvent Enhanced Valorization of Bamboo for Concurrent Bioethanol and Carbon Dot Production

Sicheng Jin , Yongan Meng , Dongtian Miao , Chun Shi , Jing Yang , Zhengjun Shi , Hai-Yan Yang *

Posted Date: 28 April 2026

doi: 10.20944/preprints202604.1958.v1

Keywords: bamboo; deep eutectic solvent; delignification; enzymatic saccharification; bioethanol

 doi:10.20944/preprints202604.1958.v1

Article

Ternary Choline Chloride–Monoethanolamine Based Deep Eutectic Solvent Enhanced Valorization of Bamboo for Concurrent Bioethanol and Carbon Dot Production

Sicheng Jin, Yongan Meng, Dongtian Miao, Chun Shi, Jing Yang, Zhengjun Shi and Hai-Yan Yang *

College of Material and Chemical Engineering, Southwest Forestry University, Kunming 650224, China

* Correspondence: yanghaiyan@swfu.edu.cn; Tel.: +86-0871-63863105

Abstract

Efficient pretreatment is essential for improving the conversion of lignocellulose into fermentable sugars and bioethanol. In this study, choline chloride–monoethanolamine (ChCl-MEA)-based ternary deep eutectic solvents containing H_2O_2, $NaHCO_3$, Na_2S, or ethylene glycol were prepared and applied to pretreatment of *Dendrocalamus brandisii*. Among the tested systems, ChCl-MEA-Na_2S showed the best overall pretreatment performance, achieving 92.8% delignification and 86.1% cellulose retention. It also effectively disrupted lignin–carbohydrate associations, reduced lignin shielding and generated a more accessible cellulose-rich substrate for bioconversion. In the following separation enzymatic hydrolysis and fermentation, 92.2% cellulose in substrate was conversed to glucose and 17.49 g/L ethanol was obtained via the fermentation of enzymatic hydrolysate. Taking the bioconversion of substrate into consideration, the ChCl-MEA-H_2O_2 and ChCl-MEA-Na_2S were recovered for full components utilization. Especially, the carbon dots produced from the degradation compounds in ChCl-MEA-H_2O_2 DESs had favorable antioxidation and antibacterial performance due to the oxygen-containing group caused by oxidation of H_2O_2.

Keywords: bamboo; deep eutectic solvent; delignification; enzymatic saccharification; bioethanol

1. Introduction

The increasing depletion of fossil resources and the growing concern over environmental pollution have accelerated the search for renewable feedstocks for sustainable energy and chemical production [1]. Lignocellulosic biomass, as the most abundant renewable organic carbon resource on Earth, is mainly composed of cellulose, hemicellulose, and lignin, and has great potential for the production of biofuels, biochemicals, and advanced biomaterials [2]. However, the compact and recalcitrant cell-wall architecture of lignocellulose, which is governed by extensive hydrogen bonding, lignin–carbohydrate associations, and hydrophobic interactions, severely restricts its efficient fractionation and subsequent valorization [3]. Conventional pretreatment methods, such as dilute acid, alkali, and organic solvent treatments, can improve biomass deconstruction to some extent, but they often suffer from harsh operating conditions, equipment corrosion, solvent recovery burdens, and undesirable degradation of biomass components, which limit their green and high-value applications [4].

Deep eutectic solvents (DESs) have emerged as a promising class of green and designable solvents for lignocellulosic biorefineries [5]. In general, DESs are formed through intermolecular interactions between hydrogen bond acceptors and hydrogen bond donors, and they usually exhibit low volatility, tunable physicochemical properties, facile preparation, and relatively low cost [6]. Compared with conventional volatile organic solvents and, in some cases, ionic liquids, DES systems

 doi:10.20944/preprints202604.1958.v1

have shown considerable potential for selectively disrupting interactions within plant cell walls and promoting the fractionation of cellulose, hemicellulose, and lignin under relatively mild conditions [7]. In recent years, DES-based pretreatment and fractionation strategies have been increasingly explored for biomass conversion. Properly designed DESs can facilitate cellulose enrichment, promote hemicellulose and lignin removal, and improve the downstream conversion efficiency of lignocellulosic feedstocks [8]. Meanwhile, DESs can strongly influence lignin extraction behavior, condensation tendency, and the physicochemical properties of the recovered lignin. Thus, DESs also provide attractive platforms for lignin valorization in integrated biorefinery [9,10]. Among the DESs systems, basic DESs show less efficiency in delignification but high hemicellulose preservation [11,12].

whereas the role of functional third components in regulating the microenvironment of alkaline ChCl-MEA systems and their subsequent influence on residue interfacial properties, enzyme-substrate interactions, ethanol production, and spent-liquor utilization remains insufficiently clarified. In particular, a direct comparison of oxidative, alkaline, reductive, and hydrogen-bond-regulating third components within the same ChCl-MEA framework can provide useful insight into the structure-function relationship of ternary DESs for bamboo biorefinery.

Therefore, in this study, H_2O_2, $NaHCO_3$, Na_2S, and ethylene glycol (EG) were introduced into a choline chloride–monoethanolamine (ChCl-MEA) DES system for pretreatment of bamboo. The effects of a third component on the physicochemical properties of ChCl-MEA DES systems were investigated. The efficiency of the modified DES pretreatment was assessed based on biomass fractionation, cellulose accessibility, enzymatic saccharification, ethanol fermentation, and recovered liquor valorization. This work aims to establish a clearer link between third-component regulation, substrate structural reconstruction, and bioethanol-oriented bamboo conversion, while also exploring carbon-dot preparation as an auxiliary pathway for spent-liquor valorization.

2. Materials and Methods

2.1. Materials

Dendrocalamus brandisii was collected from the bamboo garden of Southwest Forestry University. The raw material was naturally air-dried, pulverized, and sieved to 40–60 mesh prior to use. Choline chloride (ChCl, ≥98%), monoethanolamine (MEA, ≥99.5%), hydrogen peroxide solution (H_2O_2, 30 wt%), sodium bicarbonate ($NaHCO_3$, ≥99.5%), sodium sulfide nonahydrate ($Na_2S{\cdot}9H_2O$, ≥98%), and ethylene glycol (EG, ≥99.5%) were purchased from Sinopharm Group Co., Ltd. (China). Commercial cellulase preparations Cellic CTec2 (200 FPU/mL) and Celluclast 1.5L (40 mg/mL) were obtained from Sigma-Aldrich (Shanghai, China). *Saccharomyces cerevisiae* used for ethanol fermentation was purchased from Angel Yeast Co., Ltd. (Yichang, China). *Escherichia coli* (*E. coli*) and *Staphylococcus aureus* (*S. aureus*) strains used for antibacterial assays were obtained from Beijing Baochang Biotechnology Co., Ltd.

2.2. Preparation and Characterization of DESs

The ChCl-MEA (CM) deep eutectic solvent was prepared by mixing choline chloride and monoethanolamine at a molar ratio of 1:6. For the ternary deep eutectic solvents (TDESs), H_2O_2, $NaHCO_3$, Na_2S and EG were individually added to the ChCl-MEA DES system as the third component, with a molar ratio of 0.2 relative to the ChCl. Then, the mixtures were magnetically stirred in a water bath at 80 °C until a transparent, homogeneous liquid was formed.

The Kamlet–Taft parameters (α, β, and π^*) of the DESs were determined using the solvatochromic probes 4-nitroaniline, N,N-diethyl-4-nitroaniline, and Nile Red according to Xue et al. [13]. To provide a molecular-level interpretation of the interactions between DESs and lignocellulosic components, representative computational analyses were performed. The molecular structures were geometrically optimized using ORCA 4.0 software at the B3LYP-D3(BJ)/def2-SVP level of theory [14]. Electrostatic potential (ESP), reduced density gradient (RDG), hydrogen-bonding tendency, and interaction-energy analyses were conducted to compare the interaction characteristics

 doi:10.20944/preprints202604.1958.v1

of different DES systems with lignocellulosic model compounds. The ESP and RDG results were analyzed using Multiwfn [15], and the noncovalent interaction regions were visualized using VMD software [16]. Veratryl glycerol-*β*-guaiacyl ether (VG), 4-O-methylglucurono-xylan, and cellobiose were selected as representative model compounds for lignin, hemicellulose, and cellulose, respectively [17]. These computational results were used as qualitative support for interpreting the different interaction tendencies of the DES systems.

2.3. Pretreatments

For the pretreatment step, the pretreatment temperature was first optimized. Briefly, 10 g of DB powder was mixed with 100 g of ChCl-MEA, and the mixture was incubated in an oil bath at 120 °C, 130 °C, and 140 °C for 3 h, respectively. Pretreatments using TDESs were performed at 140 °C for 3 h. At end of the reaction, the solid residue was collected by filtration and successively washed with 300 mL of acetone/water (1:1, v/v) and hot deionized water until the filtrate approached neutral pH. The resulting cellulose-rich solids were dried, labeled according to temperature or the third component as CM-X (X). The filtrate was adjusted to pH 2 with hydrochloric acid to precipitate lignin, which was then collected by centrifugation. The supernatant was concentrated by rotary evaporation to remove water and recover the DESs for carbon dots (CDs) production.

For CDs preparation, the recovered ChCl-MEA-H_2O_2 and ChCl-MEA-Na_2S were diluted to a 10 wt% aqueous solution and transferred into a Teflon-lined stainless-steel autoclave, and heated at 180 °C for 12 h. After cooling to room temperature, the obtained dispersion was centrifuged, filtered through a 0.22 μm membrane, and dialyzed against deionized water before further characterization. The obtained CDs were labeled as CD-CM-H_2O_2 and CD-CM-Na_2S, respectively.

2.4. Enzymatic Hydrolysis and Fermentation

Enzymatic hydrolysis was performed in sodium citrate buffer (pH 4.8) at a solids loading of 5% (w/v). Cellic CTec2 was dosed at 15 FPU/g substrate, and the reaction was conducted at 50 °C with shaking at 150 rpm for 72 h; hydrolysates were withdrawn periodically during the process. At end of the enzymatic saccharification, the hydrolysates were filtered and sterilized at 121 °C prior to inoculation with *Saccharomyces cerevisiae*. Fermentation was carried out at 35 °C with shaking at 90 rpm for 24 h, and supernatant samples were collected at intervals for ethanol analysis. Glucose, xylose, and ethanol concentrations during enzymatic hydrolysis and fermentation were quantified using high-performance liquid chromatography (HPLC, Agilent 1260, USA) equipped with a Bio-Rad Aminex HPX-87H column. A 5 mM H_2SO_4 aqueous solution was used as the mobile phase at a flow rate of 0.6 mL/min, and the column temperature was maintained at 55 °C [18]. Glucose and xylose yields were calculated based on the carbohydrate contents of the corresponding substrates, and ethanol output in the mass balance was normalized to 100 g of raw bamboo.

2.5. Characterization

The composition of samples was determined in accordance with the NREL LAP protocol [18]. The hydrophobicity and enzyme accessibility of the cellulosic substrates were evaluated by Rose Bengal and Direct Red 28 staining, respectively [19,20]. The degree of polymerization (DP) of cellulose was calculated based on its intrinsic viscosity in a cupriethylenediamine (CED) solution [21]. The protein adsorption behavior of Celluclast 1.5 L (40 mg/mL protein content) on the samples was analyzed using the Langmuir adsorption isotherm model [22]. The maximum adsorption capacity (Γm) and adsorption affinity constant (K) were obtained from Langmuir fitting, and the adsorption strength parameter R was calculated from Γm and K.

The specific surface area of the raw and pretreated samples was measured by Brunauer-Emmett-Teller (BET) analysis using an ASAP 2460 surface area analyzer (Micromeritics Instrument Ltd., USA). The crystallinity index (CrI) of the raw and pretreated bamboo samples was determined by X-ray diffraction (XRD), and the relative change in crystallinity was expressed as the ratio of CrI to

 doi:10.20944/preprints202604.1958.v1

cellulose content (CrI/cellulose content). The surface elemental composition of the cellulosic substrates and CDs was analyzed by X-ray photoelectron spectroscopy (XPS, Thermo Scientific, USA) to determine the distribution of carbon and oxygen, as well as to calculate the surface coverage of lignin. Functional groups in the cellulosic substrates were characterized by Fourier transform infrared spectroscopy (FT-IR) over the wavenumber range of 4000-400 cm^{-1}.

The optical properties of CDs were investigated using a UV-Vis and a fluorescence spectrophotometer. The CDs were dispersed in deionized water until their optical density in the range of 300-400 nm was below 0.10, so as to minimize the inner filter effect. Subs-quently, the absorption spectra of the CDs dispersions in the range of 200-600 nm were recorded on a UV-Vis spectrophotometer at room temperature with an interval of 1 nm. The fluorescence spectra of CDs were measured using a fluorescence spectrophotometer. The excitation wavelength was scanned from 310 to 380 nm with a step size of 10 nm, and the emission spectra in the range of 400-600 nm were recorded at each excitation wavelength. Both the excitation and emission slit widths were set to 5 nm, the scanning rate was 200-300 nm/min, and the photomultiplier tube voltage was adjusted to avoid signal saturation. The excitation/emission pair corresponding to the maximum emission intensity was defined as the optimal excitation/emission wavelength.

Before antioxidant and antibacterial assays, the purified CD dispersions were adjusted to a concentration of 1.0 mg/mL. The antioxidant activity of the CDs was evaluated by 2,2-diphenyl-1-picrylhydrazyl (DPPH) and 2,2′-azinobis(3-ethylbenzothiazoline-6-sulfonic acid) (ABTS) radical scavenging assays [23,24]. The antibacterial performance was assessed by the agar well diffusion method on Mueller-Hinton agar plates, using S. aureus and E. coli as the test strains [25]. Briefly, bacterial suspensions were adjusted to approximately 10^6 CFU/mL and uniformly spread onto the agar plates. Wells with a diameter of 2 mm were punched into the agar, and 100 μL of CD dispersion was added to each well, followed by incubation at 37 °C for 24 h.

All experiments were performed in triplicate, and the mean values with corresponding standard deviations were calculated.

3. Results and Discussion

3.1. Effect of Pretreatment on Structural Characteristics of Bamboo

3.1.1. Chemical Composition

Deep eutectic solvents are robust solvents for biomass fractionation, prioritizing delignification while preserving cellulose. As depicted in Figure 1, the chemical composition of bamboo and its derived residues undergoes dramatic changes upon pretreatment. Raw bamboo contains 52.4% cellulose, 14.4% xylans, and 25.3% lignin. Treatment with ChCl-MEA results in significant delignification (from 67.1% to 85.9%) and cellulose enrichment (from 52.4% to 70.8%) as temperatures rose from 120 °C to 140 °C, albeit with a marginal decline in solid recovery (71.0% to 67.0%). The outstanding delignification efficiency is likely due to the facilitated solvent penetration into the cell wall at higher temperatures, which concomitantly accelerates the degradation of ether linkages within lignin and LCCs [26,27]. However, 85.6% to 87.8% xylans retention are achieved during pretreatment, demonstrating the efficacy of this alkaline DES system in hemicellulose preservation [28].

Compared with the binary system, the introduction of a third component further improves the fractionation performance of ChCl-MEA and promots lignocellulose deconstruction effectively at 140 °C. Among the ternary DESs, ChCl-MEA-Na_2S achieves the highest delignification rate (92.8%), while ChCl-MEA-EG (90.7%) and ChCl-MEA-$NaHCO_3$ (90.6%) also shows favorable lignin removal efficiencies, all outperforming ChCl-MEA-H_2O_2 (85.8%). The superior performance of the Na_2S-containing system can be attributed to the strong nucleophilicity and mild reducing character of sulfide species (HS^- and S^{2-}), which can promote *β-O*-4 ether bond cleavage through thiolysis-like reactions while suppressing lignin condensation and redeposition. The addition of Na_2S therefore provides ChCl-MEA with a stronger nucleophilic, reductive, and alkaline microenvironment, which

 doi:10.20944/preprints202604.1958.v1

is favorable for delignification [29]. By contrast, the H_2O_2 system relies mainly on radical oxidation and may cause partial polysaccharide degradation; $NaHCO_3$ provides moderate basicity and has a limited effect on ether bond cleavage; and EG mainly acts as a co-solvent to regulate viscosity, with relatively weak chemical reactivity [30]. Overall, ChCl-MEA-Na_2S exhibits the most pronounced pretreatment effect at 140 °C, giving a solid recovery of 59.0% and the recovered solid containing 76.5% cellulose, 19.4% xylan, and 3.1% lignin.

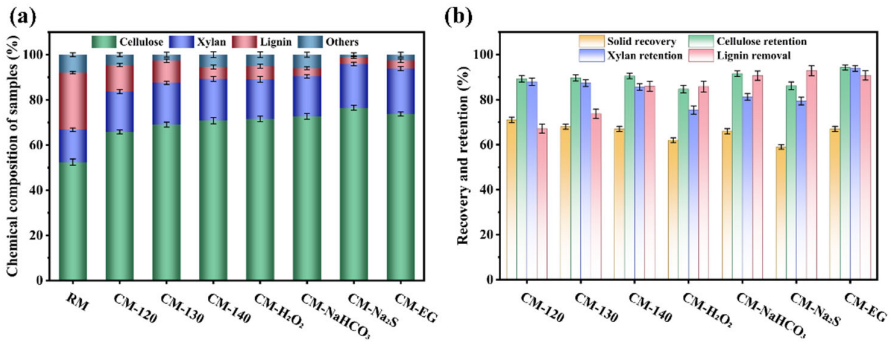

Figure 1. Changes in the chemical composition of bamboo residues after DES pretreatment. (**a**) Solid recovery, cellulose, xylan, and lignin contents of residues obtained from binary ChCl-MEA pretreatment at 120, 130, and 140 °C. (**b**) Comparison of residue composition and delignification performance for ternary ChCl-MEA-based DES systems at 140 °C.

The changes of chemical composition are also confirmed by FT-IR and XPS (Figures 2 and S1). The intensity of peak at 1730 cm^{-1} decreases after pretreatment indicating removal of hemicellulose. Meanwhile, the decline in intensity of peak at 1519 cm^{-1} confirmed delignification of DESs pretreatment [31] (Figure S1). Consisting with chemical composition, delignification leads to decrease of content in C–C/C–H groups from 34.0% to 24.6%, and increase of O/C ratio from 0.413 to 0.490 as increasing pretreatment temperature from 120 to 140 ºC. The surface lignin coverage also decreases from 78.7% to 63.8% with increment of pretreatment temperature. These changes indicate that increasing pretreatment severity progressively reduced lignin shielding at the residue surface and promoted the exposure of oxygen-containing polysaccharide-related functionalities [32]. Coordination with the third component, the O/C ratio further increases but differs with the properties of the third component. CM-H_2O_2 and CM-$NaHCO_3$ exhibit O/C ratios of 0.489 and 0.500, together with surface lignin coverages of 65.2% and 62.4%, respectively, indicating more oxygenated and less lignin-covered surfaces than those of the corresponding binary residues. CM-Na_2S has the highest O/C ratio (0.507) and the lowest surface lignin coverage (59.6%), confirming that this system most effectively reduces surface lignin shielding. In contrast, CM-EG shows an O/C ratio of 0.466, while its surface lignin coverage remains at 68.9% and the C–C/C–H contribution roses to 42.8%. This discrepancy between bulk delignification and surface composition suggests that dissolved lignin fragments are partially re-deposited on the outer surface during post-treatment [33,34]. Among the ternary systems, the Na_2S-containing DES generates the most favorable surface characteristics for reducing lignin shielding, whereas the EG-containing system retains a more lignin-enriched outer layer that could hinder enzyme accessibility.

 doi:10.20944/preprints202604.1958.v1

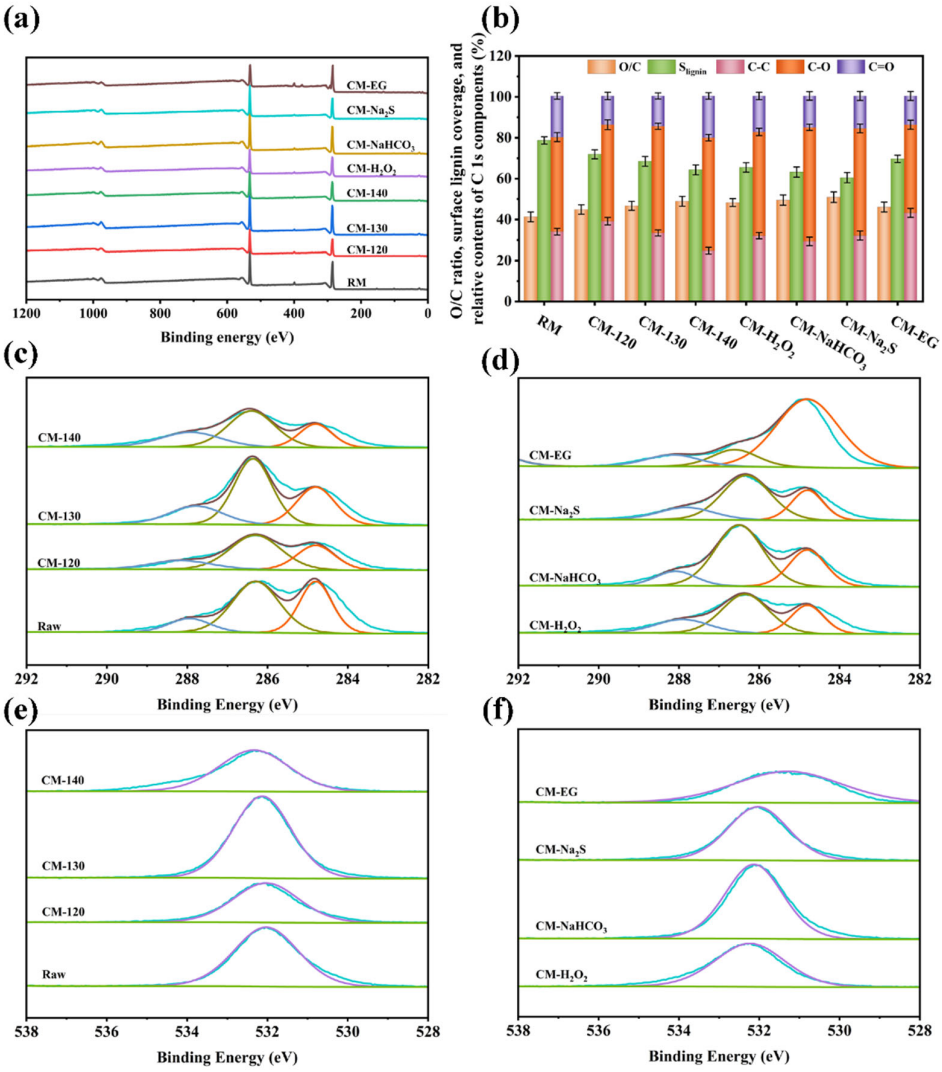

Figure 2. XPS characterization of raw bamboo and DES-pretreated residues. (**a**) XPS survey spectra of raw and pretreated samples. (**b**) XPS-derived O/C ratio, surface lignin coverage, and relative contents of C 1s components. (**c**,**d**) High-resolution C 1s spectra of residues obtained from the binary and ternary DES systems, respectively. (**e**,**f**) High-resolution O 1s spectra of residues obtained from the binary and ternary DES systems, respectively.

3.1.2. Changes in Degree of Polymerization and Crystalline Structure

DES pretreatment not only alters the chemical composition of bamboo residues, but also affects the structure of cellulose. Figure 3 depicts the effect of DESs pretreatments on the degree of polymerization (DP) and crystalline index of samples. The DP of raw bamboo is 1788, which decreases to 1488 (CM-120), 1125 (CM-130), and 1022 (CM-140) after binary ChCl-MEA pretreatment, indicating that cellulose chains are progressively cleaved as the pretreatment severity increased. In the ternary systems, this trend becomes more pronounced: the DP further decreases to 852 for CM-H_2O_2, 713 for CM-$NaHCO_3$, and 492 for CM-Na_2S, whereas CM-EG still retains a relatively higher value of 1099. The decrease in DP indicates that DES treatment weakened the constraints between cellulose chains, making the chain segments more relaxed and exposed, while also further opening the originally compact internal structure of the substrate. Among all the systems, CM-Na_2S shows the lowest DP, suggesting that this ChCl-MEA-Na_2S caused the most extensive disruption of the bonding structures within the bamboo cell wall [35], which is consistent with its higher delignification efficiency and stronger enzymatic hydrolysis performance.

 doi:10.20944/preprints202604.1958.v1

XRD spectra reflect the changes in the ordered structure of cellulose. All samples retain the characteristic diffraction peaks of cellulose I at around 18.8° and 22.5°, indicating that DESs pretreatments do not alter the cellulose crystal form. Considering that the apparent crystallinity increases passively with the removal of lignin and hemicellulose, the *CrI* to cellulose content ratio was further used for normalized comparison. The raw bamboo exhibits a *CrI*/Cellulose value of 1.028, which decreases to 0.957 (CM-120), 0.925 (CM-130), and 0.922 (CM-140) after binary ChCl-MEA pretreatment, suggesting that the internal ordered hydrogen-bonding network is partly disturbed. In the ternary systems, this value further decreases to 0.884 (CM-H_2O_2), 0.861 (CM-EG), 0.828 (CM-$NaHCO_3$), and 0.812 (CM-Na_2S). The more pronounced decreases observed for the $NaHCO_3$ and Na_2S systems indicates a stronger disruption of the highly ordered cellulose regions, which is more favorable for chain swelling and substrate opening [36]. Taken together with the DP results, DESs pretreatments promote cellulose chain scission also weaken the ordered packing within its supramolecular structure, and this effect was most pronounced in the ChCl-MEA-Na_2S system.

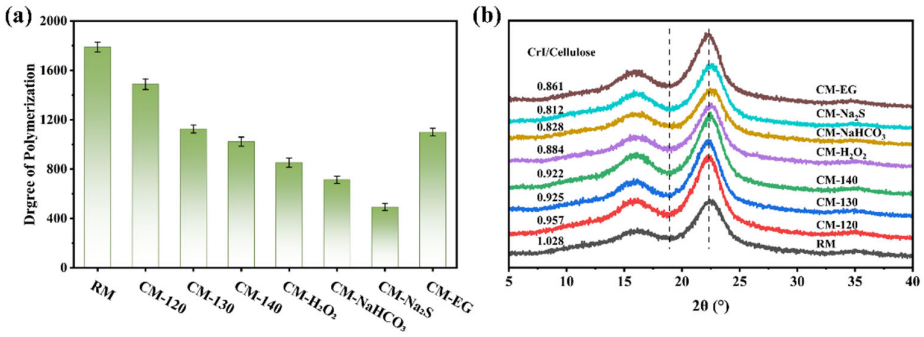

Figure 3. Changes in cellulose degree of polymerization (**a**) and crystalline structure of bamboo residues (**b**) after DES pretreatment.

3.1.3. Specific Surface Area, Hydrophobicity, and Enzyme–Substrate Interactions

The changes in the intrinsic structure of cellulose also affect interfacial properties of samples. After pretreatment, the specific surface area, hydrophobicity, cellulose accessibility, and enzyme adsorption behavior of samples are shown in Figure 4. BET analysis shows that pretreatment with ChCl-MEA increase specific surface area of samples from 1.019 m²/g to 1.362 m²/g (CM-120), 1.635 m²/g (CM-130), and 2.086 m²/g (CM-140), respectively, indicating that the cell-wall structure is gradually loosened and generates accessible pores as the pretreatment severity increased. In the ternary systems, the specific surface area further increases to 2.268 m²/g (CM-H_2O_2), 2.584 m²/g (CM-$NaHCO_3$), and 3.024 m²/g (CM-Na_2S), and 1.776 m²/g (CM-EG), respectively.

Correspondingly, the cellulose accessibility increases markedly from 44.3 mg/g for raw bamboo to 59.5 mg/g (CM-120), 90.8 mg/g (CM-130), and 128.2 mg/g (CM-140), respectively. In the ternary systems, it further increases to 161.4 mg/g (CM-H_2O_2), 142.5 mg/g (CM-$NaHCO_3$), and 182.7 mg/g (CM-Na_2S), while CM-EG shows 113.7 mg/g. The increase in cellulose accessibility is much greater than the increase in specific surface area, indicating that enzyme access to the substrate was governed not only by pore enlargement, but also by cellulose chain relaxation, reduced lignin shielding, and improved interfacial chemical properties.

The hydrophobicity results further reveal the changes in the surface properties of the residues. The hydrophobicity of raw bamboo is 34.3 L/g, which decreases to 17.5 L/g (CM-120), 11.6 L/g (CM-130), and 6.7 L/g (CM-140) after binary ChCl-MEA pretreatment. In the ternary systems, it further decreases to 4.8 L/g (CM-H_2O_2), 5.4 L/g (CM-$NaHCO_3$), and 3.2 L/g (CM-Na_2S), whereas CM-EG shows 7.1 L/g. The decrease in hydrophobicity indicates that the lignin-rich hydrophobic domains on the substrate surface are reduced, while polar groups became more exposed, thereby improving interfacial wettability. This change could not only facilitate enzyme access to the substrate, but also weaken the non-productive adsorption caused by residual lignin [37].

 doi:10.20944/preprints202604.1958.v1

Structural and interfacial changes reflect the enzyme adsorption behavior. For raw bamboo, the maximum adsorption capacity (*Γ*m), affinity constant (K), and R value are 15.4 mg/g, 4.4 mL/mg, and 0.068 L/g, respectively. After binary ChCl-MEA pretreatment, *Γ*m increases to 15.9, 19.1, and 20.8 mg/g, K increases to 7.8, 8.5, and 8.4 mL/mg, and R increases to 0.124, 0.162, and 0.175 L/g for CM-120, CM-130, and CM-140, respectively. In the ternary systems, *Γ*m reaches 23.7, 22.7, and 26.5 mg/g for CM-H_2O_2, CM-$NaHCO_3$, and CM-Na_2S, with corresponding K values of 10.1, 7.7, and 10.3 mL/mg and R values of 0.239, 0.175, and 0.273 L/g, respectively; CM-EG shows 21.6 mg/g, 7.5 mL/mg, and 0.162 L/g.

Overall, the ChCl-MEA-Na_2S pretreatment exhibits highest effect on specific surface area, cellulose accessibility and enzyme adsorption capacity and affinity among all DESs pretreatments. The pore opening, surface hydrophilization, and exposure of reactive sites boost the enzyme–substrate interactions, which will enhance the saccharification efficiency of cellulose [38].

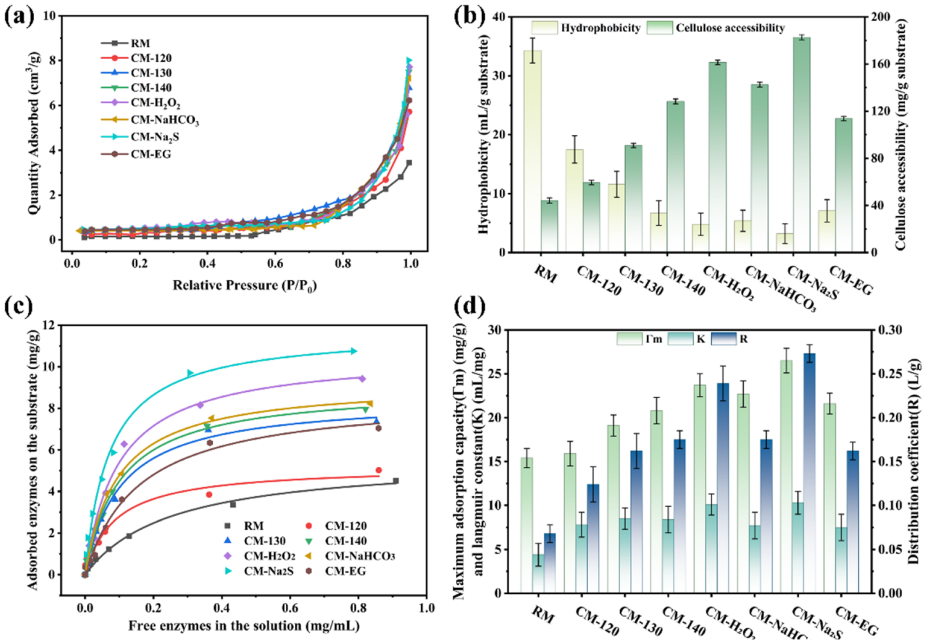

Figure 4. Changes in the interfacial and enzymatic properties of bamboo residues after DES pretreatment. (**a**) BET specific surface area. (**b**) Surface hydrophobicity and cellulose accessibility of raw and pretreated residues. (**c**) Langmuir adsorption isotherms of cellulase on raw and pretreated residues. (**d**) Langmuir adsorption behavior of cellulase on raw and pretreated residues.

3.2. Effect of Pretreatment on Cellulose Saccharification and Bioethanol Production

Effect of pretreatments on enzymatic saccharification of cellulose and bioethanol production is depicted in Figures 5 and S2. Without pretreatment, the glucose and xylose yields of RM via enzymatic hydrolysis are only 22.4% and 27.6%, respectively, indicating that the dense lignin–hemicellulose matrix in native bamboo severely limits the action of enzymes on the polysaccharide fraction. After pretreatment with the binary ChCl-MEA, the glucose yield increases to 58.3% (CM-120) 76.3% (CM-130), 74.9% (CM-140). The xylose yield increases to 84.9% (CM-120), 97.2%(CM-130) and 97.3%(CM-140). These results suggest that increasing the pretreatment severity can markedly improve the enzyatic sacchrification efficiency of carbohydrate fractions. Pretreatment with ternary DES systems further enhanced cellulose conversion. The yields of glucose from CM-H_2O_2, CM-EG, CM-$NaHCO_3$, and CM-Na_2S via enzymatic hydrolysis are 87.4%, 72.3%, 82.8%, and 92.2%, respectively. while the corresponding ethanol concentrations were 15.63, 11.95, 13.66, and 17.49 g/L. The high bioconversion of samples obtained from pretreatment with ternary DESs is ascribed to the enhancement in specific surface area, cellulose accessibility and enzyme adsorption capacity and

 doi:10.20944/preprints202604.1958.v1

affinity of substrates. Among these samples, the substrate pretreated with ChCl-MEA-Na_2S DES at 140 ºC possesses excellent bioconversion capability.

Taking 100 g bamboo into account, enzymatic hydrolysis of RM obtained 14.4 g glucose and 13.1 g xylose. Ferments these reduce sugars obtains 3.7 g ethanol. Pretreatment with ChCl-MEA at 140 ºC recovers 45.1 g cellulose, 11.4 g xylans and 1.8 g lignin, respectively. Enzymatic hydrolysis the substrate obtains 35.6 g glucose and 11.9 g xylose, and 13.9 g ethanol is generated via fermentation. Coordination Na_2S in to ChCl-MEA further improve the digestibility of substrate, and yields 17.2 g ethanol through separate enzymatic hydrolysis and fermentation.

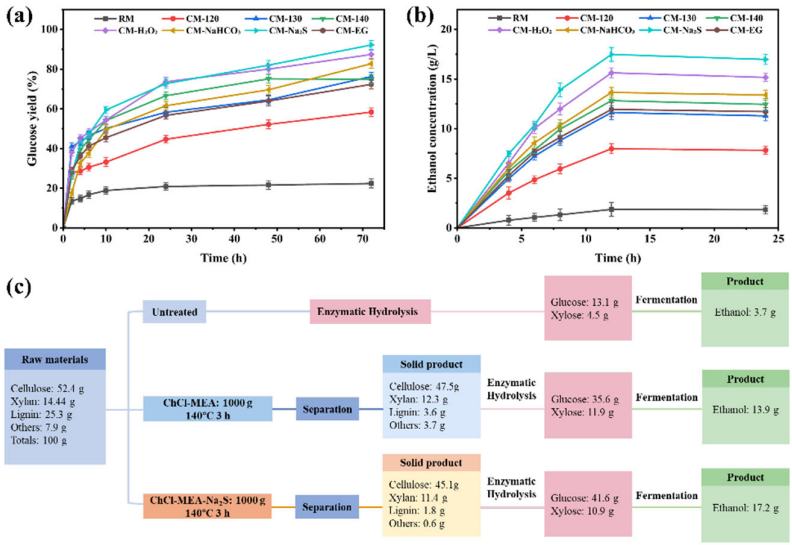

Figure 5. Enzymatic saccharification and ethanol fermentation performance of raw and DES-pretreated bamboo. (**a**) Glucose yields after enzymatic hydrolysis. (**b**) Ethanol concentration after fermentation. (**c**) Mass balance of bamboo conversion after DES pretreatment, enzymatic hydrolysis, and ethanol fermentation.

3.3. Molecular Interpretation of Ternary DES Performance

To further understand the interactions between DESs and lignocellulosic substrate, RDG-based noncovalent interaction analysis, molecular electrostatic potential (MEP), hydrogen-bond statistics, Kamlet-Taft parameters, and NMR were performed and shown in Figures 6 and S3-5. The Kamlet–Taft parameters of ChCl-MEA are $\alpha = 1.05$, $\beta = 0.51$, $\pi^* = 0.93$, respectively. The and viscosity of ChCl-MEA are 11.7, and 4.8 mPa·s. Coordination with Na_2S increases the acidity, basicity and polarity (α = 1.12, $\pi^* = 1.42$, $\beta = 0.54$, pH = 12.3), indicating a more polarized and strongly basic environment. ChCl-MEA-$NaHCO_3$ shows relatively high polarity with $\pi^* = 1.35$ and pH = 12.4, while ChCl-MEA-H_2O_2 exhibited the highest α value of 1.58, suggesting stronger hydrogen-bond donor ability.

As shown in Figure 6, all DESs exhibit obvious attractive interaction regions, confirming that hydrogen bonding and electrostatic interactions are the major forces stabilizing the eutectic systems. The H_2O_2-containing system shows a relatively uniform enhancement of attractive regions, suggesting an overall increase in polarity, whereas the $NaHCO_3$-containing system displays more localized asymmetry. The Na_2S-containing DES exhibits the most concentrated and strongest attractive regions, indicating the formation of a more strongly polarized local microenvironment. By contrast, the EG-containing DES shows a limited enhancement, implying that its role is more closely related to hydrogen-bond reorganization than to strong chemical activation. The MEP results further support these differences. For binary ChCl-MEA, the minimum and maximum electrostatic potentials are -53.80 and +38.38 kcal/mol, respectively. After introducing H_2O_2, the minimum negative potential deepens to -64.55 kcal/mol and the maximum positive potential increases to +58.11 kcal/mol, indicating a stronger contrast between electron-rich and electron-deficient regions and thus a greater tendency to interact with polar carbohydrate groups. In the $NaHCO_3$ system, the minimum negative

 doi:10.20944/preprints202604.1958.v1

potential is -43.26 kcal/mol, whereas the maximum positive potential rises to +79.51 kcal/mol, reflecting a more asymmetric local electric field. The Na_2S system shows the highest maximum positive potential (+103.99 kcal/mol), while the minimum negative potential remains at about -55.00 kcal/mol, indicating that it could generate the strongest potential gradient around aryl-ether bonds and favorable for activating and cleaving lignin-related linkages. In contrast, the EG system shows a weaker enhancement in polarity, suggesting that EG contributes mainly to viscosity reduction, swelling promotion, and hydrogen-bond reorganization rather than direct bond cleavage [39]. The hydrogen-bond and cumulative interaction-energy statistics in are also consistent with these results: H_2O_2 and EG show stronger interactions in the carbohydrate-related models, whereas Na_2S exhibit the highest cumulative interaction energy in the Axyl-VG model, indicating a stronger directed interaction with lignin aromatic ether structures.

This interpretation is also supported by the NMR results. As shown in Figure S4, the ^1H and ^{13}C NMR spectra of the recovered DESs retain the main characteristic signals of the fresh systems, with no obvious new backbone peaks or disappearance of the original peaks, indicating that the main DES framework is still preserved after pretreatment. However, broadening and variations of peak intensity appears around the 3-4 ppm, suggesting rearrangement of the local hydrogen-bonding environment. In addition, the intensity of cross-peaks in the δ 2.5-4.0 ppm region decreases after pretreatment, suggesting decrease in hydrogen-bond intensity and reconstruction of hydrogen-bonds [40]. Further evidence is provided by the 2D NOESY spectra (Figure S5). Compared with the fresh DESs, the recovered systems still retain identifiable intermolecular cross-peaks, although the cross-peak intensity becomes weaker and more dispersed after pretreatment, indicating that the DES framework is preserved while the spatial proximity and hydrogen-bonding network are reorganized to different extents. In all, the excellent pretreatment performance of DESs ChCl-MEA-Na_2S and ChCl-MEA-H_2O_2 is due to the enhancement of polarity, hydrogen-bond capacity.

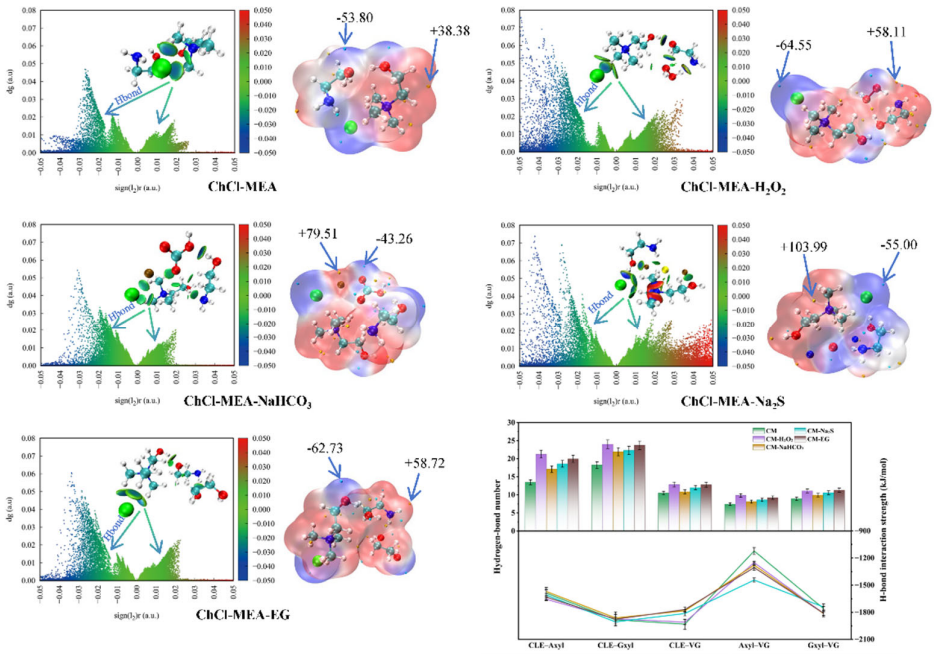

Figure 6. RDG isosurfaces, molecular electrostatic potential (MEP) distributions, and hydrogen-bond number and cumulative interaction energy analyses of ChCl-MEA and ternary DES systems.

3.4. Structure and Properties of Carbon Dots (CD) Prepared from Recovered DESs

Due to the high fractionation performance of DESs ChCl-MEA-H_2O_2 and ChCl-MEA-Na_2S systems, the degraded components of bamboo in these DESs are conversed to carbon dots for full

 doi:10.20944/preprints202604.1958.v1

utilization of lignocellulosic biomass. Both CDs exhibit well-dispersed quasi-spherical morphologies at the nanoscale. The average particle size of the carbon dots derived from the ChCl-MEA-H_2O_2 and ChCl-MEA-Na_2S system are 2.95 nm and 3.47 nm, respectively (Figure 7a). The lattice spacings of the CD-CM-H_2O_2 and CD-CM-Na_2S are 0.204 and 0.208 nm, close to the spacing of graphitic carbon (100), suggesting that both samples possessed a certain degree of ordered carbon structure. The slightly larger lattice spacing in the Na_2S-derived carbon dots may be due to the condensation of lignin in CD-CM-Na_2S DES, which lead to defect or local structural disorder [41].

The functional groups on surface of CDs are detected via XPS analysis and shown in Figure 7b. C and O are as the main elements in CDs, and C-C/C=C, C-O, and O-C=O are the main bonds on CDs surface. Compared with the CD-CM-Na_2S, higher proportion of oxygen-containing species is observed in CD-CM-H_2O_2, indicating a stronger degree of surface oxidation [42].

In terms of optical properties (Figure 7c), both samples show obvious absorption peaks in the range of 200-300 nm, corresponding to π-π* transitions in the carbon framework, while the absorption tails at longer wavelengths are associated with surface defect states and n-π* transitions. Fluorescence measurements show that both carbon dots exhibited emission peaks near 450 nm, but the sample derived from the H_2O_2 system shows higher fluorescence intensity, indicating that its surface-state distribution and defect structure are more favorable for fluorescence emission.

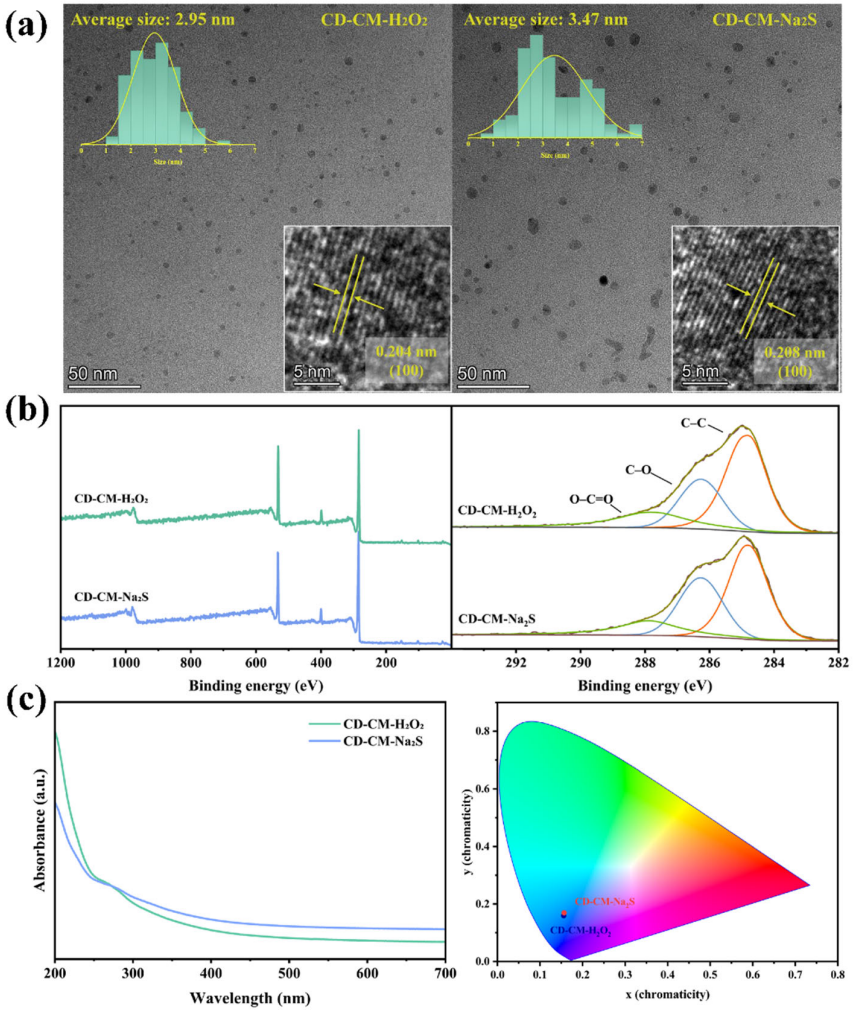

Figure 7. (a) Electron microscopy images of carbon dots. (**b**) XPS and related surface-chemical characterization of carbon dots. (**c**)UV-Vis absorption and fluorescence emission behaviors of carbon dots.

 doi:10.20944/preprints202604.1958.v1

The functional groups on surface also contribute to bioactivity of CDs. The DPPH and ABTS radical-scavenging rates of the H_2O_2-derived carbon dots reach 85.2% and 93.7%, respectively, which were higher than those of the Na_2S-derived sample (75.9% and 88.3%). This indicates that the former possessed stronger antioxidant activity, which may be related to its smaller particle size and higher content of surface oxygen-containing functional groups [43,44]. In the antibacterial tests, the Na_2S-derived carbon dots produces inhibition zones of 2 mm against both *S. aureus* and *E. coli*, whereas the H_2O_2-derived sample produced inhibition zones of 5 and 4 mm, respectively, indicating stronger antibacterial activity. These results suggest that the degradation component from lignocellulosic biomass during DESs pretreatments can be serves as carbon sources for carbon-dot preparation. The physiochemical properties of CDs are also related to the properties of DESs. In all, the recovered ChCl-MEA-H_2O_2 DES after pretreatment is favorite for active CDs production due to the oxidation of H_2O_2.

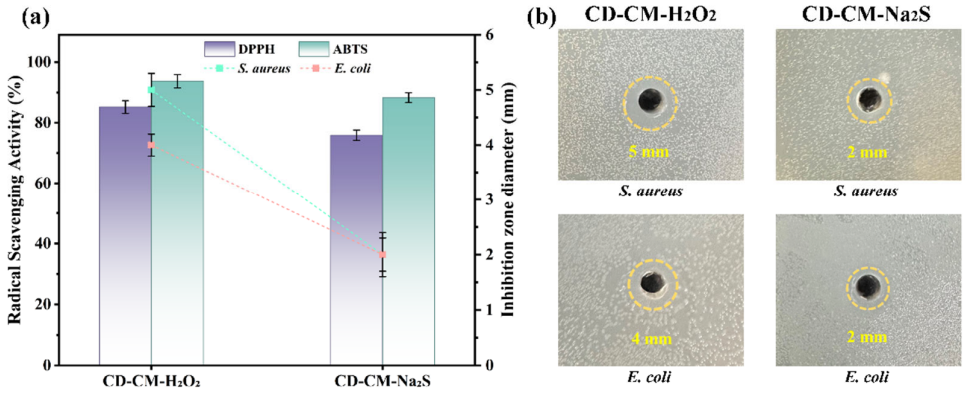

Figure 8. Bioactivities of carbon dots. (**a**) Radical-scavenging activities evaluated by DPPH and ABTS assays. (**b**) Antibacterial activity against *S. aureus* and *E. coli*.

4. Conclusions

This study demonstrates that the lignin dissolution and cellulose preservation during ChCl-MEA-based DES pretreatment can be effectively enhanced by the third-component Multiscale characterizations and molecular simulation revealed that the enhanced performance stemmed from stronger disruption of lignin-carbohydrate complexes (LCCs), improved cellulose accessibility, reduced lignin shielding, and favorable enzyme-substrate interactions. Among the tested systems, ChCl-MEA-Na_2S pretreatment at 140 °C for 3 h showed the best overall performance, affording 92.8% delignification, 92.2% cellulose saccharification, and a 17.2 g per 100 g raw bamboo ethanol yield. After pretreatment, the degradation components in DESs were converted into carbon dots, providing an auxiliary valorization route for macromolecule-derived byproducts.

Supplementary Materials: The supporting information includes supplementary FT-IR spectra (Figure S1), yields of xylose via enzymatic hydrolysis (Figure S2), physicochemical-property characterization of DESs systems (Figures S3-S5).

Author Contributions: Sicheng Jin: Methodology, Investigation, Resources, Writing - original draft. Yongan Meng: Resources, Validation, Writing - original draft. Dongtian Miao: Methodology, Investigation, Data curation. Chun Shi: Data curation, Writing - review & editing. Jing Yang: Methodology, Resources, Conceptualization, Writing - review & editing. Zhengjun Shi: Data curation, Formal analysis, Writing - original draft. Hai-Yan Yang: Supervision, Conceptualization, Writing - review & editing. #Yongan Meng contributed equal to Sichen Jin.

 doi:10.20944/preprints202604.1958.v1

Funding: This research was funded by the National Natural Science Foundation of China, grant number 32260369, and the Xing Dian Youth Talents Support Program of Yunnan Province, grant number XDYC-QNRC-2022-0175.

Data Availability Statement: The data presented in this study are available from the corresponding author upon reasonable request.

Acknowledgments: The authors thank the Yunnan Provincial Key Laboratory of Wood and Bamboo Biomass Materials for providing experimental support.

Conflicts of Interest: The authors declare that they have no known competing financial interests or personal relationships that could have appeared to influence the work reported in this paper.

References

1. Hansen, B.B.; Spittle, S.; Chen, B.; Poe, D.; Zhang, Y.; Klein, J.M.; Horton, A.; Adhikari, L.; Zelovich, T.; Doherty, B.W.; et al. Deep eutectic solvents: A review of fundamentals and applications. *Chem. Rev.* **2021**, 121, 1232-1285. https://doi.org/10.1021/acs.chemrev.0c00385
2. Smith, E.L.; Abbott, A.P.; Ryder, K.S. Deep eutectic solvents (DESs) and their applications. *Chem. Rev.* **2014**, 114, 11060-11082. https://doi.org/10.1021/cr300162p
3. Beluhan, S.; Mihajlovski, K.; Šantek, B.; Ivančić Šantek, M. The production of bioethanol from lignocellulosic biomass: Pretreatment methods, fermentation, and downstream processing. *Energies* **2023**, 16, 7003. https://doi.org/10.3390/en16197003
4. Morán-Aguilar, M.G.; Costa-Trigo, I.; Ramírez-Pérez, A.M.; de Blas, E.; Calderón-Santoyo, M.; Aguilar-Uscanga, M.G.; Domínguez, J.M. Development of sustainable biorefinery processes applying deep eutectic solvents to agrofood wastes. *Energies* **2022**, 15, 4101. https://doi.org/10.3390/en15114101
5. Suriyachai, N.; Khongchamnan, P.; Laosiripojana, N.; Kreetachat, T.; Wongcharee, S.; Sakulthaew, C.; Chokejaroenrat, C.; Imman, S. Optimization of cellulose recovery using deep eutectic solvent fractionation: A response surface method approach. *Energies* **2024**, 17, 4257. https://doi.org/10.3390/en17174257
6. Kim, K.H.; Eudes, A.; Jeong, K.; Yoo, C.G.; Kim, C.S.; Ragauskas, A.J. Integration of renewable deep eutectic solvents with engineered biomass to achieve a closed-loop biorefinery. *Proc. Natl. Acad. Sci. USA* **2019**, 116, 13816-13824. https://doi.org/10.1073/pnas.1904636116
7. Hong, S.; Shen, X.-J.; Xue, Z.; Sun, Z.; Yuan, T.-Q. Structure-function relationships of deep eutectic solvents for lignin extraction and chemical transformation. *Green Chem.* **2020**, 22, 7219-7232. https://doi.org/10.1039/D0GC02439B
8. Luo, Z.; Qian, Q.; Sun, H.; Wei, Q.; Zhou, J.; Wang, K. Lignin-first biorefinery for converting lignocellulosic biomass into fuels and chemicals. *Energies* **2023**, 16, 125. https://doi.org/10.3390/en16010125
9. Díaz-González, A.; Perez Luna, M.Y.; Ramírez Morales, E.; Saldaña-Trinidad, S.; Rojas Blanco, L.; de la Cruz-Arreola, S.; Pérez-Sariñana, B.Y.; Robles-Ocampo, J.B. Assessment of the pretreatments and bioconversion of lignocellulosic biomass recovered from the husk of the cocoa pod. *Energies* **2022**, 15, 3544. https://doi.org/10.3390/en15103544
10. Ekwe, N.B.; Tyufekchiev, M.V.; Salifu, A.A.; Schmidt-Rohr, K.; Zheng, Z.; Maag, A.R.; Tompsett, G.A.; Cai, C.M.; Onche, E.O.; Ates, A.; et al. Bamboo as a cost-effective source of renewable carbon for sustainable economic development in low- and middle-income economies. *Energies* **2023**, 16, 331. https://doi.org/10.3390/en16010331
11. Yu, X.; Fan, K.; Wang, K.; Jiang, J.; Peng, X.; Yang, H.; Wang, M. Physicochemical variation of the main components during wild pretreatment process based on the concept of the whole utilization of bamboo. *Energies* **2021**, 14, 6857. https://doi.org/10.3390/en14216857
12. Yao, Z.; Huang, W.; Wu, D. Deep eutectic solvent pretreatment and green separation of lignocellulose: A review. *Appl. Sci.* **2024**, 14, 7662. https://doi.org/10.3390/app14177662
13. Teles, A.R.R.; Capela, E.V.; do Carmo, R.S.; Coutinho, J.A.P.; Silvestre, A.J.D.; Freire, M.G. Solvatochromic parameters of deep eutectic solvents formed by ammonium-based salts and carboxylic acids. *Fluid Phase Equilib.* **2017**, 448, 15-21. https://doi.org/10.1016/j.fluid.2017.04.020

 doi:10.20944/preprints202604.1958.v1

14. Neese, F. Software update: The ORCA program system, version 4.0. *WIREs Comput. Mol. Sci.* **2018**, 8, e1327. https://doi.org/10.1002/wcms.1327
15. Johnson, E.R.; Keinan, S.; Mori-Sánchez, P.; Contreras-García, J.; Cohen, A.J.; Yang, W. Revealing noncovalent interactions. *J. Am. Chem. Soc.* **2010**, 132, 6498-6506. https://doi.org/10.1021/ja100936w
16. Lu, T.; Chen, F. Multiwfn: A multifunctional wavefunction analyzer. *J. Comput. Chem.* **2012**, 33, 580-592. https://doi.org/10.1002/jcc.22885
17. Grimme, S.; Ehrlich, S.; Goerigk, L. Effect of the damping function in dispersion corrected density functional theory. *J. Comput. Chem.* **2011**, 32, 1456-1465. https://doi.org/10.1002/jcc.21759.
18. Sluiter, A.; Hames, B.; Ruiz, R.; Scarlata, C.; Sluiter, J.; Templeton, D.; Crocker, D. *Determination of structural carbohydrates and lignin in biomass*; NREL/TP-510-42618; National Renewable Energy Laboratory: Golden, CO, USA, 2012. https://www.nrel.gov/docs/gen/fy13/42618.pdf
19. Wiman, M.; Dienes, D.; Hansen, M.A.T.; van der Meulen, T.; Zacchi, G.; Lidén, G. Cellulose accessibility determines the rate of enzymatic hydrolysis of steam-pretreated spruce. *Bioresour. Technol.* **2012**, 126, 208-215. https://doi.org/10.1016/j.biortech.2012.08.082
20. Gessner, A.; Waicz, R.; Lieske, A.; Paulke, B.R.; Mäder, K.; Müller, R.H. Nanoparticles with decreasing surface hydrophobicities: Influence on plasma protein adsorption. *Int. J. Pharm.* **2000**, 196, 245-249. https://doi.org/10.1016/S0378-5173(99)00432-9
21. TAPPI T 230 om-99. *Viscosity of pulp (capillary viscometer method)*. TAPPI Press: Atlanta, GA, USA, 1999. https://webstore.ansi.org/standards/tappi/230-1127430
22. Lu, X.; Zheng, X.; Li, X.; Zhao, J. Adsorption and mechanism of cellulase enzymes onto lignin isolated from corn stover pretreated with liquid hot water. *Biotechnol. Biofuels* **2016**, 9, 118. https://doi.org/10.1186/s13068-016-0531-0
23. Brand-Williams, W.; Cuvelier, M.E.; Berset, C. Use of a free radical method to evaluate antioxidant activity. *LWT - Food Sci. Technol.* **1995**, 28, 25-30. https://doi.org/10.1016/S0023-6438(95)80008-5
24. Re, R.; Pellegrini, N.; Proteggente, A.; Pannala, A.; Yang, M.; Rice-Evans, C. Antioxidant activity applying an improved ABTS radical cation decolorization assay. *Free Radic. Biol. Med.* **1999**, 26, 1231-1237. https://doi.org/10.1016/S0891-5849(98)00315-3
25. Balouiri, M.; Sadiki, M.; Ibnsouda, S.K. Methods for in vitro evaluating antimicrobial activity: A review. *J. Pharm. Anal.* **2016**, 6, 71-79. https://doi.org/10.1016/j.jpha.2015.11.005
26. Segal, L.; Creely, J.J.; Martin, A.E.; Conrad, C.M. An empirical method for estimating the degree of crystallinity of native cellulose using the X-ray diffractometer. *Text. Res. J.* **1959**, 29, 786-794. https://doi.org/10.1177/004051755902901003
27. Humphrey, W.; Dalke, A.; Schulten, K. VMD: Visual molecular dynamics. *J. Mol. Graph.* **1996**, 14, 33-38. https://doi.org/10.1016/0263-7855(96)00018-5
28. Zhang, L.; Yu, H.; Liu, S.; et al. Kamlet-Taft parameters of deep eutectic solvents and their relationship with dissolution of main lignocellulosic components. *Ind. Eng. Chem. Res.* **2023**, 62, 11723-11734. https://doi.org/10.1021/acs.iecr.3c01309
29. Liu, X.; Cheng, J.; Huang, C.; Wang, J.; Fang, G.; Shen, K.; Meng, X.; Ragauskas, A.J. Alkali-facilitated deep eutectic solvent for effective bamboo saccharification. *Bioresour. Technol.* **2023**, 367, 128297. https://doi.org/10.1016/j.biortech.2022.128297
30. Huo, D.; Sun, Y.; Yang, Q.; et al. Selective degradation of hemicellulose and lignin via deep eutectic solvent pretreatment to improve enzymolysis efficiency. *Bioresour. Technol.* **2023**, 376, 128937. https://doi.org/10.1016/j.biortech.2023.128937
31. Feng, Y.; Eberhardt, T.L.; Meng, F.; Xu, C.; Pan, H. Efficient extraction of lignin from moso bamboo by microwave-assisted ternary deep eutectic solvent pretreatment for enhanced enzymatic hydrolysis. *Bioresour. Technol.* **2024**, 400, 130666. https://doi.org/10.1016/j.biortech.2024.130666
32. Luo, L.; Yuan, X.; Zhang, S.; Wang, X.; Li, M.; Wang, S. Effect of pretreatments on the enzymatic hydrolysis of high-yield bamboo chemo-mechanical pulp by changing the surface lignin content. *Polymers* **2021**, 13, 787. https://doi.org/10.3390/polym13050787

 doi:10.20944/preprints202604.1958.v1

33. Hou, Q.; Liu, Z.; Shi, Z.; Yang, H.; Wang, D.; Yang, J. A deep eutectic solvent pretreatment with self-cleaning lignin droplets to efficiently improve enzymatic saccharification and ethanol production of bamboo residues. *Ind. Crops Prod.* **2024**, 216, 118730. https://doi.org/10.1016/j.indcrop.2024.118730
34. Chen, T.; Guo, G.; Shen, D.; Tang, Y. Metal salt-based deep eutectic solvent pretreatment of moso bamboo to improve enzymatic hydrolysis. *Fermentation* **2023**, 9, 618. https://doi.org/10.3390/fermentation9070618
35. Pan, X.; Liu, Y.; Ma, Z.; Qin, Y.; Lu, X.; Feng, X.; Shao, Q.; Zhu, Y. Molecular insight into the mechanism of lignin dissolution in acid choline chloride-based deep eutectic solvents. *J. Mol. Liq.* **2024**, 406, 125123. https://doi.org/10.1016/j.molliq.2024.125123
36. Ma, Y.; Liu, Z.; Lei, L.; Hu, S.; Hou, Y. Mechanism insights for the roles of hydrogen bonds on the dissolution and separation of lignin in LA-ChCl system. *Ind. Crops Prod.* **2024**, 222, 119911. https://doi.org/10.1016/j.indcrop.2024.119911
37. Liu, X.; Zhang, J.; Fang, Y.; Wu, H.; Yang, H. Investigation of a Na_2S-assisted deep eutectic solvent pretreatment for enhanced saccharification and high-quality lignin. *Ind. Crops Prod.* **2024**, 208, 117790. https://doi.org/10.1016/j.indcrop.2023.117790
38. Meng, F.; Eberhardt, T.L.; Li, Y.; Xu, C.; Pan, H. Assessment of the interaction mechanisms for a novel ternary deep eutectic solvent developed to enhance the enzymatic hydrolysis of bamboo. *Bioresour. Technol.* **2025**, 433, 132737. https://doi.org/10.1016/j.biortech.2025.132737
39. Meng, F.; Fan, J.; Cui, F.; et al. Hydrogen peroxide-citric acid pretreatment of bamboo residues for enhanced enzymatic hydrolysis and ethanol production. *Bioresour. Technol.* **2023**, 383, 129230. https://doi.org/10.1016/j.biortech.2023.129230
40. Delso, I.; Lafuente, C.; Muñoz-Embid, J.; Artal, M. NMR study of choline chloride-based deep eutectic solvents. *J. Mol. Liq.* **2019**, 290, 111236. https://doi.org/10.1016/j.molliq.2019.111236
41. Zhao, R.; Sheng, Y.; Yang, H.; Shi, Z.; Wang, D.; Yang, J. Tailored bamboo fractionation with ternary deep eutectic solvent system to maximize biorefinery toward enzymatic saccharification and lignin recovery. *Int. J. Biol. Macromol.* **2025**, 308, 142361. https://doi.org/10.1016/j.ijbiomac.2025.142361
42. Yao, L.; Chai, M.; Cui, P.; et al. Mechanism of enhanced enzymatic hydrolysis performance by ethanol assisted deep eutectic solvent pretreatment: From the perspective of lignin. *Bioresour. Technol.* **2023**, 385, 129461. https://doi.org/10.1016/j.biortech.2023.129461
43. Wang, R.; Zhang, S.; Zhang, J.; Wang, J.; Bian, H.; Jin, L.; Zhang, Y. State-of-the-art of lignin-derived carbon nanodots: Preparation, properties, and applications. *Int. J. Biol. Macromol.* **2024**, 273, 132897. https://doi.org/10.1016/j.ijbiomac.2024.132897
44. Qu, X.; Gao, C.; Fu, L.; Chu, Y.; Wang, J.H.; Qiu, H.; Chen, J. Positively charged carbon dots with antibacterial and antioxidant dual activities for promoting infected wound healing. *ACS Appl. Mater. Interfaces* **2023**, 15, 18608-18619. https://doi.org/10.1021/acsami.2c21839